

# Improved, Real-time Artifact Detection and Reacquisition for Diffusion Tensor Imaging (DTI)

Y. Li<sup>1,2</sup>, S. M. Shea<sup>2,3</sup>, H. Jiang<sup>3</sup>, C. H. Lorenz<sup>2,3</sup>, and S. Mori<sup>3</sup>

<sup>1</sup>Biomedical Engineering, Johns Hopkins University School of Medicine, Baltimore, MD, United States, <sup>2</sup>Center for Applied Medical Imaging, Siemens Corporate Research, Baltimore, MD, United States, <sup>3</sup>Russell H. Morgan Department of Radiology and Radiological Sciences, Johns Hopkins University School of Medicine, Baltimore, MD, United States

**Introduction:** In DTI, diffusion tensor is estimated by least square error fit of measured diffusion weighted images (DWI) and b0 images. However, DWIs often suffer from pulsation-caused, subpixel motion artifacts which result in erroneous tensor estimation. To solve this problem, outlier rejection methods, such as RESTORE [1][2], have been proposed in which a tensor is first estimated with all data points using robust fitting, then data points with large fitting errors are rejected as outliers, and finally, a tensor calculation without the rejected points is performed. However, this approach becomes unstable when there are multiple outliers because the initial fitting starts to dissociate from the real value, compromising its ability to accurately measure the amount of errors. To solve this problem, we added an additional weighing term to the robust fitting cost function based on slice-by-slice intensity discontinuity. This new term is based on anatomical consistency and, thus, is a criterion independent to the fitting procedure. In this presentation, we first tested improvement in outlier detection accuracy by adding the new term. This method was then implemented into Siemens MR Image Calculation Environment (ICE) software so that corrupted slices can be reacquired in real-time.

**Methods:** In RESTORE[2], robust fitting is based on a weighted least square fit procedure which tries to minimize a cost function  $\sum_i w_i r_i^2$ , where  $r_i$  is the error term on the  $i$ th diffusion direction,  $w_i = 1/(r_i^2 + C^2)$  is the weighting term, and the normalization factor  $C$  is the median absolute deviation (MAD) of set  $\{r_i, i=1,2,\dots,\# \text{of diffusion directions}\}$ . With the weighting term, the fitting is less affected by points with large error. Our proposed new index is called Inter-Slice Intensity Discontinuity (ISID). When multi-slice axial 2D images are viewed from the sagittal or coronal views (Fig.1(a)), the artifact usually appears as intensity discontinuity along the axial (z) direction. We devised a method to extract this information as follows. First, a close operation [3] on z direction was applied to raw DWI (Fig.1(b)) and the difference between the images with and without the operation was calculated as an ISID image. Second, to cancel effects of inherent anatomical changes, the ISID image of each DWI was subtracted from the ISID of average DWI, which led to the final ISID that could highlight the artifactual intensity discontinuity clearly (Fig.1(c)). The weighting factor with the ISID term becomes  $w_i = 1/(r_i^2 + C^2) \cdot 1/(id_i^2 + c^2)$ , where  $id$  is the ISID and normalization factor  $c$  is the MAD of all ISID values.

Levenberg-Marquardt method is used for the optimization and the initial value for the robust fitting is from standard linear fitting. Pixels with large error values are marked, and after a clustering procedure, the clusters with the number of marked pixels above a threshold (30 pixels) are defined as artifact. We compared our method and RESTORE on data sets from 5 pediatric patients. Each subject was imaged twice with a single-shot, diffusion-weighted EPI sequence on a Siemens Avanto 1.5T scanner. Imaging parameters were as follows: TR: 3700-7700ms (depends on number of slices); TE: 80-93ms; matrix = 80x80 (FOV = 160x160 mm) or 96x96 (200x200 mm); slice thickness = 2.0-2.2 mm; 50-60 contiguous slices; and b value=800 s/mm<sup>2</sup> in 12 directions. An expert identified slices that contained artifacts in only one of the two repeated scans such that the subtraction could be used as the gold standard to define artifact points. A Receiver Operator Curve Analysis (ROC) for each artifact detection method was done by changing the threshold of fitting error for rejecting outliers and then calculating specificity and sensitivity as compared to the gold standard.

For the real-time monitoring, the above algorithm was implemented into the Siemens ICE software on a 3T Tim-Trio scanner. Images were processed online and rejected slices were reacquired after completion of the initial data set in real-time. The sequence was tested on a human subject with a single-shot, diffusion-weighted EPI sequence with the following parameters: TR/TE = 6800/104ms; matrix = 128x128 (FOV = 200x200 mm); slice thickness = 5 mm; 35 slices; and b value = 1000 s/mm<sup>2</sup> in 20 directions.

**Results:** From the pediatric patients, 21 slice positions (with one to four corrupted DWIs per slice position) were used for the ROC analysis (Fig. 2). Our method outperformed RESTORE consistently in all slices while the difference becomes more obvious as the number of corrupted DWIs increases. For the real-time artifact detection sequence, 14 slices were rejected and then reacquired in a single subject. Fig.3(a) shows one of the rejected slices with artifact while the reacquired image (Fig.3(c)) is artifact free.

**Discussions and Conclusion:** We demonstrated that the ISID information improves the performance of automated artifact detection algorithm. Excluding corrupted data points in tensor estimation helps improving accuracy of offline diffusion tensor calculation. However, offline quality control has one major drawback: lowered SNR in the resulting tensor estimation. Our implementation of real-time outlier rejection and reacquisition shows that this is a more ideal approach that can ensure the required number of data points even after data rejection.

**Acknowledgement:** This study is supported by RO1AG20012 / P41RR15241. Siemens Corporate Research provided funding for an internship for the first author to support this work.

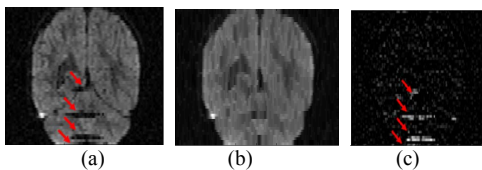


Fig.1 Illustration of ISID. (a): a coronal view of an axial multi-slice DWI data with artifacts (red arrows), (b): after the close operation, (c): the ISID image

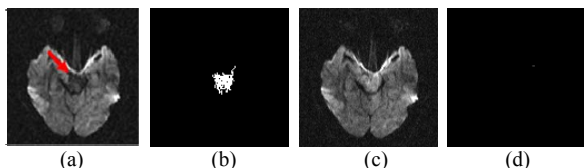


Fig.3 An example of the real-time quality control; (a): rejected image; (b): a detected outlier pixel cluster in the rejected image; (c) automatically reacquired image; (d) no outlier pixel cluster detected in reacquired image.

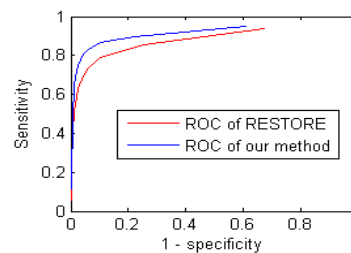


Fig.2 ROCs of the offline test; blue: proposed method; red: RESTORE

## References

- [1] LC Chang, DK Jones and C Pierpaoli, MRM 53:1088-1095
- [2] M Niethammer, S Bouix, S Aja-Fernandez, etc., MICCAI 2007
- [3] ER. Dougherty, J Astola, An Introduction to Nonlinear Image Processing, SPIE press, 1994